Regular Article

Impact of aeration strategies on fed-batch cell culture kinetics in a single-use 24-well miniature bioreactor☆

J.P.J. Betts [a], S.R.C. Warr [b], G.B. Finka [b], M. Uden [b], M. Town [a], J.M. Janda [a], F. Baganz [a], G.J. Lye [a,*]

[a] The Advanced Centre for Biochemical Engineering, Department of Biochemical Engineering, University College London, Torrington Place, London WC1E 7JE, UK
[b] BioPharm R&D, BioPharm Process Research, GlaxoSmithKline R&D, Stevenage SG1 2NY, UK

ARTICLE INFO

ABSTRACT

The need to bring new biopharmaceutical products to market more quickly and to reduce final manufacturing costs is driving early stage, small scale bioprocess development. This work describes a comprehensive engineering characterisation of a novel, single-use 24-well parallel miniature bioreactor system. Cell culture performance is also investigated, with particular focus on the aeration strategies adopted at this small scale (7 mL) either by headspace sparging alone or by direct gas sparging into the culture medium.

Apparent volumetric oxygen mass transfer coefficient (k_La) values ranged between 3–22 h^{-1} and 4–53 h^{-1} for headspace aeration and direct gas sparging respectively. The higher k_La values with direct gas sparging correlated directly with the increase in gas–liquid interfacial area per unit volume. Mixing times (t_m) over a range of conditions were generally in the range 1–13 s and decreased with increasing shaking frequency (500–800 rpm). Direct gas sparging also served to reduce t_m values by a factor of up to 19 fold.

The impact of aeration strategies on cell culture kinetics of a model CHO cell line was also determined. Cultures performed with head space aeration alone showed the highest viable cell density (VCD) (15.2×10^6 cells mL^{-1}), viability retention and antibody titre (1.58 g L^{-1}). These were greater than in conventional shake flask cultures due to the improved control of the μ24 bioreactor system. In all cases the miniature bioreactor managed good control of process parameters such as pH 6.95 ± 0.4, temperature $T°C$ 37 ± 0.4 and DO% 57 ± 32. Cultures performed with direct gas sparging showed a 25–45% reduction in VCD (depending on the aeration strategy used) and a similar reduction in antibody titre. Overall this work shows the successful application of the miniature bioreactor system for industrially relevant fed-batch cultures and highlights the impact of the dispersed gas phase on cell culture performance at the small scale.

1. Introduction

Biopharmaceuticals are attracting significant commercial interest because of enhanced success rates in clinical trials (30%) compared to conventional pharmaceuticals (21.5%) [1]. To date, the most successful biopharmaceuticals have been monoclonal antibodies (mAbs) and it is estimated that a further 30% of new drugs licensed in the next decade will be based on antibody molecules [2].

From an engineering perspective, the ability to construct common manufacturing platforms [3,4] for a range of such antibody products has been a key factor driving industrial interest in antibody based therapeutics.

Increased demand for antibody products has prompted industry to increase production capacity by construction of bulk manufacturing facilities and to improve cell culture processes to raise product titres [3]. However, product uptake is hindered by high selling prices. Sikora [5] reports prices of up to £70,000 per patient per year in the UK for some monoclonal antibody therapies. Accordingly, there is pressure from governments and health authorities to decrease biopharmaceutical selling prices which increases the industrial incentive for cost-effective manufacture of these products [6]. To meet such pressures and yet remain economically viable, companies must find ways to accelerate R&D programmes and increase bioprocess efficiency.

Nomenclature

a	area, mm^2
CD-CHO	chemically defined CHO cell line media
CHO	Chinese hamster ovary derived cell line
C_P	normalised dissolved oxygen concentration, %
$dhfr^{-/-}$	dihydrofolate reductase deficient cell line
d_f	inner diameter of shaken vessel, m
d_o	orbital shaking diameter, m
d_w	microwell diameter, m
DO	dissolved oxygen (%)
h_L	displaced liquid height, mm
IVC	integral of viable cell concentration, $\times 10^6$ cells mL^{-1} day^{-1}
$k_L a$	volumetric oxygen mass transfer coefficient, h^{-1}
$k_L a_{app}$	apparent volumetric oxygen mass transfer coefficient, h^{-1}
mAb	monoclonal antibody
MTX	methotrexate
N	shaking frequency, s^{-1}
OD	optical density
P	power input, W
PBS	phosphate buffered saline
PERC	non-direct gas sparged plate design for use with the μ24 bioreactor
Ph	phase number (as defined in Eq. 3), dimensionless
PPG media	Proprietary production growth media
Qp	cell specific productivity, pg $cell^{-1}$ day^{-1}
REG	direct gas sparged plate design for use with the μ24 bioreactor
RO	reverse osmosis
SRW	standard round well microtitre plate
STR	stirred tank bioreactor
t	time, s
t_{mt}	mass transfer time, $k_L a^{-1}$, s
t_m	mixing time, s
V	liquid volume, m^3
VCD	viable cell density, $\times 10^6$ cells mL^{-1}
v/v	concentration, volume by volume
VVM	gas volume flow per unit of liquid volume per minute
wv	working volume

Greek letters

ρ	density, $kg\,m^{-3}$
τ_P	probe response time, s

Biopharmaceuticals are ultimately manufactured at large scale; however here there is limited opportunity to perform process development and optimisation. Consequently most companies have validated scale-down models of their pilot and manufacturing scale bioreactors [7]. These usually take the form of 0.5–10 L scale stirred tank bioreactors (STR) [8,9] and are used for cell culture process development. Nevertheless, there is a need for more efficient, high throughput and miniaturised bioreactors that can be used earlier during process development to further reduce time and costs. The fundamental challenge lies in creating a bioreactor model that accurately recreates the engineering environment experienced at medium and large scales in order to yield process relevant data at small scale.

A number of groups have previously demonstrated the potential to perform suspension culture of mammalian cells in shaken microwell plates [10–13]. In order to overcome the lack of control of key process parameters (e.g. pH, dissolved oxygen (DO)) in conventional plate formats a number of automated miniature bioreactor

systems have recently been commercialised. These include the μ24 bioreactor system from Pall [14,15] and the ambr™ system from TAP Biosystems (Royston, UK). Both have the ability to independently measure and control pH, DO and temperature in individual wells in parallel cell culture experiments.

The μ24 bioreactor system uses a microtitre plate format with system level control of shaking frequency and individual well control of temperature, pH and DO [14]. This work describes a comprehensive engineering analysis of the μ24 bioreactor system for fed-batch suspension culture of a model Chinese Hamster Ovary (CHO), mAb expressing cell line. In particular we show how the different aeration strategies available (surface aeration or with a dispersed gas phase) impact on fluid mixing, gas–liquid mass transfer and ultimately cell culture performance in terms of both cell growth and antibody productivity.

2. Materials and methods

2.1. Description of μ24 bioreactor platform

The μ24 bioreactor platform (MicroReactor Technologies, Pall, Port Washington, USA) has previously been described by Isett et al. [15] and Chen et al. [14]. Briefly, the μ24 consists of a single shaking base plate, with an adjustable shaking frequency from 0 to 800 rpm at a fixed 2.5 mm orbital diameter. The cell culture cassette comprises a pre-sterilised 24 deep well microtitre plate, available in PERC or REG designs as shown in Supplementary Fig. 1. Each well has a working volume (wv) of 3–7 mL. Individual wells are equipped with two thermistors that correspond to equivalent temperature monitoring and heating elements on the μ24 base plate. In addition, each well also has fluorescent pH and DO sensing patches to allow optical monitoring via LED's and detectors on the base plate. During shaking a vacuum is applied to seal the cell culture cassette to the base plate. Individual gas injection ports from the base plate feed into 0.2 μm sparge membranes within each of the wells. For the PERC plate design sparged gas passes up a central sparge tube, which is higher than the liquid surface, and therefore passes into the head space of the well to provide surface aeration only. For the REG plate design, gas is sparged directly into the base of each well creating a dispersed gas phase. Up to three different gases can be used at any one time; for mammalian cell culture purposes these will typically include an oxygen source for DO control and a carbon dioxide containing gas for pH control.

2.2. Engineering characterisation of the μ24 bioreactor

2.2.1. Oxygen mass transfer coefficient, $k_L a$ determination

The $k_L a$ values were determined experimentally using the static gassing out method as described by van't Riet [16]. All experiments were carried out at 37 °C. The fluorescent DO sensor of an individual well from a μ24 cassette (PERC or REG design) was pre-calibrated to 100% oxygen saturation in air at 37 °C. The system was operated in 'constant flow' mode, with oxygen control turned on to enable DO logging but operated such that there was no active oxygen sparging. The purge line was used to sparge test gases at defined flow rates. The test fluid was then sparged with N_2 until the DO reached zero. The required bioreactor operating conditions (shaking frequency, aeration rate, etc.) were then set and the air sparged until the probe reading reached approximately 100%. The $k_L a$ was determined taking into account the probe response time using Eq. (1) [17]:

$$C_p = \frac{1}{t_{mt} - \tau_p}\left[t_{mt}\exp\left(\frac{-t}{t_{mt}}\right) - \tau_p\exp\left(\frac{-t}{\tau_p}\right)\right] \tag{1}$$

where C_P is the normalised dissolved oxygen concentration measured by the probe at time t, t_{mt} is $1/k_L a$ and τ_P is the probe response

time. The response time of the optical probe, 18 s, was calculated by determining the time required for the DO reading to drop from 100% to below 33% by sparging the probe directly, firstly with air and then rapidly switching to N_2. Since the μ24 software contains a proprietary algorithm for averaging DO readings over time all $k_L a$ values reported here are represented as apparent, $k_L a_{app}$, values, which will slightly under predict the true $k_L a$ values. All $k_L a$ experiments were performed in triplicate.

2.2.2. Mixing time determination

Liquid phase mixing times were measured experimentally using the iodine decolourisation method as described by Bujalski et al. [18]. The brown 5 mM iodine solution (Sigma–Aldrich, Gillingham, UK, Cat No. 35089) turns colourless upon addition of an equimolar sodium thiosulphate solution (1.8 M) (Sigma–Aldrich, Cat No. S8503). Experiments were performed from either a static start with sodium thiosulphate added directly to the base of the well or with a dynamic start where sodium thiosulphate addition was made down the side of the well at a fixed position 2 cm above the liquid surface. Mixing times were quantified as described in Section 2.3 from analysis of video images as described previously [19]. All mixing time experiments were performed in triplicate.

2.2.3. Determination of evaporation levels

Specific evaporation levels from individual wells were determined based on measured changes in the concentration of a blue dye (Super Cook, Leeds, UK; at an initial concentration of 0.002%, v/v) over time. Control experiments showed that the measured increase in optical density (OD) at 630 nm was directly proportional to the reduction in liquid volume. To determine the specific well evaporation rate, a PERC plate was filled with dye stock solution (7 mL fill volume) and set in the μ24 bioreactor system at 37 °C for 9 days. Standard culture conditions were simulated by using a shaking frequency of 650 rpm and a constant purge gas flow rate of 10 mL min^{-1}. The OD was determined for each well by transferring 100 μL of sample to a standard microtitre plate and measuring the absorbance in a plate reader (Safire, Tecan, Männedorf, Switzerland). Measurements were blanked against 100 μL reverse osmosis (RO) water. Values presented here are based on triplicate measurements. The fold evaporation per well could then be calculated using Eq. (2):

$$\text{fold evaporation} = \frac{\left(A_{630,\text{final}} - A_{630,\text{blank}}\right)}{\left(A_{630,\text{initial}} - A_{630,\text{blank}}\right)} \qquad (2)$$

2.3. Visualisation of liquid phase hydrodynamics and gas–liquid dispersion

A high speed camera was used to study the liquid phase hydrodynamics, the motion and deformation of the gas–liquid surface and for bubble size and size distribution measurements. The camera used was a DVR Fastcam (Photron, California, USA). The resolution was set to 640×480 pixels for all experiments. For mixing time experiments the camera was set to record at 125 frames per second with a shutter speed of 1/frame rate. For the bubble size and distribution experiments and the surface deformation experiments the camera was set at 500 frames per second with a 1/1000 s shutter speed and twice normal gain. Image analysis was performed using ImageJ software (http://rsbweb.nih.gov/ij/). For these experiments individual wells from PERC and REG cassettes were cut from a cassette to aid visualisation and subsequent image analysis. A small Perspex box was constructed around each individual well and this was filled with glycerol so as to prevent image distortion. A chemically defined CHO cell media (CD-CHO) (Gibco, Invitrogen, Paisley, UK, Cat No. 10743-029) was used to provide a comparison to the proprietary production growth media (PPG media) used

for cell culture. Pluronic-F68 (Sigma–Aldrich, P1300) was added to RO water at 0.5 g L^{-1} to determine the effect of this component on bubble size and distribution.

For both the PERC and REG plate designs image analysis of the wells at varying shaking frequencies was performed using ImageJ to determine the displaced liquid height (h_L) and thus the area of the gas–liquid surface (a). The displaced liquid height values were determined for both plate designs at a 7 mL fill volume assuming an oval geometry. The gas sparging mechanism in the μ24 bioreactor delivers 'pulses' of gas, opening valves for 22 ms an appropriate number of times to equal the programmed gas flow rate. As such, discrete gas pulses were analysed and compared to determine reproducibility of pulses with variation of gas bubble size and number. From these values the relative gas–liquid surface area per pulse was determined. From the pulse beginning and ending frame number, and known frame rate, the average gas bubble residence time was determined. The measurement of the bubble diameter and displaced liquid height assumed that all the bubbles were spherical in order to calculate the surface area. Experiments were performed at least in triplicate.

2.4. Cell culture

2.4.1. Cell line and subculture

A model CHO DG44 dihydrofolate reductase deficient ($dhfr^{-/-}$) cell line expressing a whole IgG1 mAb product was kindly provided by GSK (Stevenage, UK). Cells were routinely passaged in a proprietary subculture medium supplemented with methotrexate (MTX) (Hanna Pharmaceutical Supply Company, Delaware, USA, Cat No. 55390-033-10) at a final concentration of 50 nM. Cells were repeatedly subcultured by dilution at 3–4 day intervals using a seeding density of 6×10^5 cells mL^{-1}. Cultures were maintained in disposable vented cap shake flasks in a Galaxy S incubator (Wolf Laboratories, York, UK) at 37 °C and 5% CO_2, on an orbital shaker (Certomat MO II, Sartorius Stedim, Aubagne, France) at a shaking frequency of 150 rpm with a 25 mm orbital diameter.

2.4.2. Fed-batch cell culture

For fed-batch experiments, cells were seeded at 8×10^5 cells mL^{-1} into a PPG media (Gibco, Invitrogen, Cat No. 041-96214V) supplemented with MTX, at a final concentration of 50 nM, and an additional proprietary amino acid solution. A standard GSK fed-batch culture protocol was followed using a single 5% (v/v) proprietary feed solution added on day 7.

Shake flask fed-batch experiments utilised disposable, vented cap 125 mL or 250 mL Erlenmeyer shake flasks (Corning Life Sciences, Amsterdam, Netherlands) with working volumes of 20–60 mL and 100–140 mL, respectively. For PERC and REG plate cultures the temperature set point of all wells was 37 °C, with an environment temperature set point of 35 °C. In addition, each well used a pH set point of 6.95 and a DO set point of 57%. All wells were sealed with a cap which has a central gas permeable filter and a check valve to limit evaporation from the culture. For cell culture with the PERC plate design enough stock inoculum was made to fill an entire plate using a 7 mL fill volume per well, in order to minimise well to well variability. Similarly, for cell culture using the REG plate design the required volume of media with Antifoam C emulsion (0.003%, v/v) (Sigma–Aldrich, Cat No. A8011) was aliquoted per well, the plate was placed into the μ24 so that the desired control set points could be reached before inoculation from one inoculum suspension. The μ24 bioreactor allows for 'active' gas flow to control pH and DO set points. There is also the ability to use a 'constant' gas flow mode which sparges a purge or background gas at a desired flow rate as well as having gases for 'active' control. PERC plates were operated using a 'constant flow' mode only whereas REG plate cultures were operated either in the 'constant
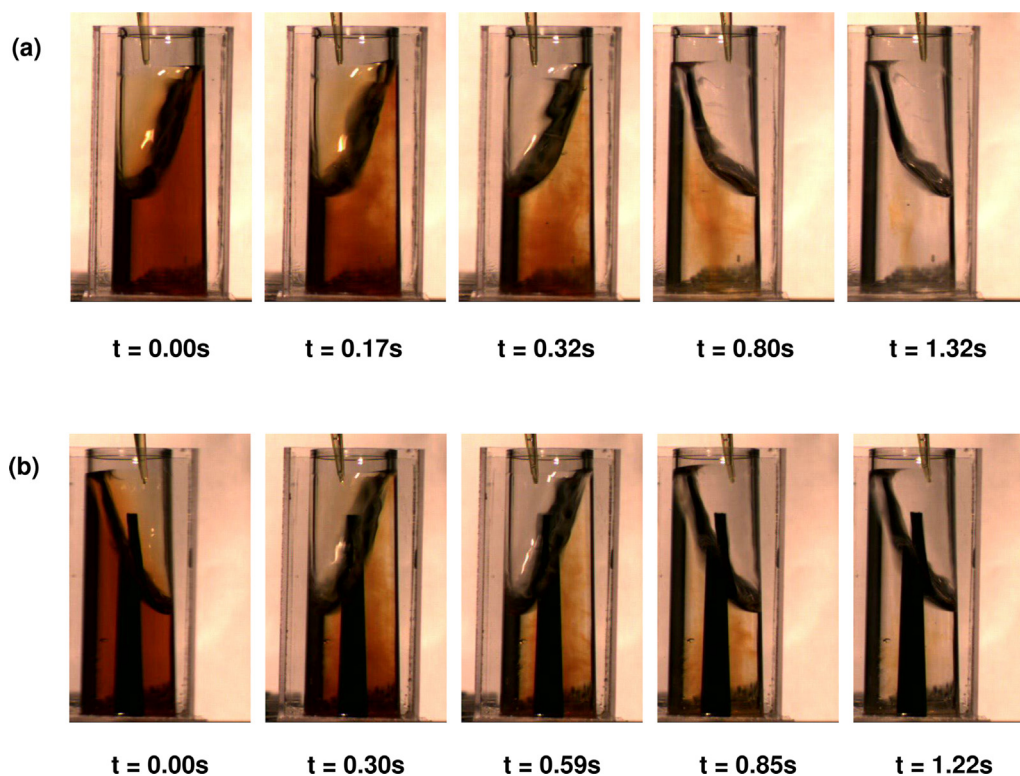
Fig. 1. Iodine decolourisation mixing time experiments for (a) PERC plate and (b) REG plate designs. Images show minimum time required to achieve complete decolourisation in each case from a dynamic start. Experimental conditions: 5 mM iodine solution; 7 mL fill volume; 800 rpm shaking frequency; d_o 2.5 mm; 25 °C.

flow' or 'active flow' modes. The μ24 operating conditions for these different cultures are shown in Supplementary Table 1.

The shaking frequencies for the μ24 fed-batch experiments were selected in order to provide a matched mixing time [20]. The cassettes were weighed at regular stages to determine the dilution factors required for the stock base feed (1 M sodium bicarbonate, 1 M sodium hydrogen carbonate) additions. Large volume inoculum additions were made using a Rainin AutoRep E (Mettler Toledo, Greifensee, Switzerland). Plate agitation was provided by an orbital microplate shaker (MS3 Digital, IKA, Staufen, Germany; agitation rate set equivalent to bioreactor operating frequency) in between individual well sampling. All experiments were carried out with 24 parallel replicates.

2.5. Analytical techniques

Viable cell density (VCD) and cell viability were determined using the Trypan Blue exclusion method using a Vi-Cell XR (Beckman Coulter, High Wycombe, UK). Samples were diluted as appropriate with TrypLE™ Express (Gibco, Invitrogen, Cat No. 12605) and incubated at 37 °C for 10 min before analysis to break up any cell clumps. Mean cell size measurements were also taken from the Vi-Cell which employs optical analysis for the measurement of cell diameter.

Metabolite analysis was performed using either a BioProfile Analyzer (Nova Biomedical, Massachusetts, USA) or a 2700 Multiparameter Bioanalytical System (YSI, Ohio, USA). In both cases samples were diluted with phosphate buffered saline as appropriate for analysis. These systems utilise immobilised enzymes in biosensor patches which enable measurement of specific dissolved metabolite levels in solution [21].

Product titre was determined based on antibody binding affinity using Protein A HPLC. The column used was a POROS® 20 micron Protein A ID Cartridge (20 μm, 2.1 mm i.d. × 30 mm, 104 μL)

(Applied Biosystems, California, USA, Cat No. 2-1001-00) on an Agilent 1100 series HPLC using Chemstation version A.0901 software (Agilent Technologies, Edinburgh, UK). The analytical protocol was 0.4 minutes of a 0.05 M sodium phosphate, 0.5 M sodium chloride buffer (pH 7.0) mobile phase to load samples followed by 3.1 min of a 0.05 M sodium phosphate, 0.5 M sodium chloride buffer (pH 2.0) mobile phase to elute samples and finally 2.5 min of the original loading buffer to regenerate the matrix; using a 1 mL min^{-1} flow rate throughout.

3. Results and discussion

3.1. Engineering characterisation of the μ24 bioreactor

3.1.1. Liquid phase hydrodynamics and mixing times

Initial experiments aimed to characterise the fluid flow in individual wells from each of the two plate designs and to quantify the liquid phase mixing times. As shown in Fig. 1, for all the shaking frequencies studied orbital shaking induced deformation of the liquid surface which then moved in an orbital motion around the walls of the well. Visually there was no difference in the nature of the fluid flow between the two plate designs.

Büchs et al. [22] discovered a phenomenon specific to shaken systems depicted by the phase number, Ph. The 'in-phase' flow regime describes conditions where the majority of the liquid circulates around the edge of the shaken vessel, synchronised with the orbital motion of the shaking platform. 'Out of phase' fluid flow occurs when only a small portion of the fluid circulates around the walls of the well with the majority of the fluid remaining stationary in the centre of the vessel [22]. The Phase number can be calculated according to Eq. (3):

$$Ph = \frac{d_o}{d_f} \left\{ 1 + 3\log_{10} \left[\frac{\rho (2\pi N) d_f^2}{4\pi} \left(1 - \sqrt{1 - \frac{4}{\pi} \left(\frac{V^{1/3}}{d_f} \right)^2} \right)^2 \right] \right\} \qquad (3)$$

Table 1

Measured liquid phase mixing times for PERC and REG plate designs from either a stationary or dynamic start. Experiments performed at 25 °C over a range of shaking frequencies and fill volumes with d_o 2.5 mm. Errors represent one standard deviation about the mean ($n = 3$).

Mixing time (s)			Shaking frequency (rpm)					
			500		650		800	
			REG	PERC	REG	PERC	REG	PERC
Fill volume (mL)	Static start	3	11 ± 1	14 ± 4	4.3 ± 0.6	4.3 ± 0.6	3.3 ± 0.6	3.0 ± 0.1
		5	31 ± 2	190 ± 34	5.0 ± 0.1	5.0 ± 0.1	4.3 ± 0.6	3.7 ± 0.6
		7	210 ± 78	3700 ± 1000	6.0 ± 0.1	6.7 ± 0.6	4.0 ± 0.1	4.0 ± 0.1
	Dynamic start	5	ND	ND	1.4 ± 0.2	1.0 ± 0.2	0.8 ± 0.10	0.8 ± 0.18
		7	13 ± 1	ND	2.0 ± 0.1	2.0 ± 0.2	1.5 ± 0.18	1.3 ± 0.16

ND: not determined.

where d_f is the inner diameter of the shaken vessel, d_o is the shaker diameter, N is the shaking frequency and V is the liquid volume [22]. For Ph > 1.26 the shaken fluid will be 'in-phase' while for Ph < 1.26 the fluid will be 'out of phase' [22]. Previously we have applied this correlation to calculate Ph for standard 24-round well plates (24 SRW), at a shaking diameter of 20 mm, fill volumes from 800 to 2000 μL and shaking frequencies from 120 to 300 rpm [10]. Under all conditions the flow of fluid was found to be 'in-phase' (Ph 8.2–12). For the μ24 system used here, assuming the liquid properties of water, Eq. (3) predicts flow conditions to be 'in-phase' for fill volumes between 3 and 7 mL and shaking frequencies above 100 rpm. This is in agreement with our visual observations.

Liquid phase mixing times were subsequently determined under non-aerated conditions. Mixing times were determined from a dynamic position, i.e. shaking platform is in operation, which is important with regards to bioreactor monitoring and control; and also from a stationary start which is unique to this bioreactor system due to the fact that the plate is removed from the shaker platform for liquid handling operations and is therefore important for initial set up, sampling, and nutrient or base feeds.

Time courses of these experiments for each plate design are illustrated in Fig. 1. Mean values of the calculated mixing times are given in Table 1. Increasing the shaking frequency and decreasing the fill volume is seen to decrease the mixing time. This is in line with results for conventional 24 SRW plates [10] where t_m values ranged from 2 to 12,900 s with fill volumes ranging from 800 to 2000 μL. Tissot et al. [23] reported t_m values below 30 s for a 1.5 L STR fitted with a single 45 mm pitched blade impeller at agitation rates between 80 and 150 rpm and Nienow reports all values below 40 s for a range of different STR configurations [24]. Thus, the t_m values reported in Table 1 are within the ranges previously reported for conventional microwell plates and at shaking frequencies above 500 rpm, are of a similar magnitude to those seen in laboratory scale bioreactors under cell culture conditions. Specifically with the PERC plate, the central sparge tube appears to retard mixing at low shaking frequencies, however, at higher shaking frequencies differences between the two well designs are not significant.

In conventional stirred tank reactors the presence of a dispersed gas phase is known to decrease liquid phase mixing times [8]. Similarly, the presence of a dispersed gas phase in the REG plate designs is seen to improve mixing as indicated in Table 2. Increasing gas flow rate leads to an almost 20-fold decrease in the mixing time. The influence of the dispersed gas phase on liquid mixing in shaken systems is particularly pronounced since the bubbles add an additional axial component to the fluid flow. In Table 2, the gas flow rates are also shown as the volumetric gas flow per unit liquid volume per minute, or VVM. This is a useful term to consider when scaling up cell culture systems. Catapano et al. [25] reports that for mammalian cell culture in stirred bioreactors the VVM should be lower than 0.1.

3.1.2. $k_L a_{app}$ determination and gas–liquid interfacial area

Apparent $k_L a$ values ($k_L a_{app}$) for both the PERC and REG plate designs are shown in Fig. 2. It is important to understand how these values vary with bioreactor operating conditions as they will influence oxygen transfer [8]. Overall, increasing shaking frequency or increasing gas flow rate increases $k_L a$. In general $k_L a_{app}$ values in the REG plate are higher and show a stronger dependency on gas flow rate than in the PERC plate. This is expected given the presence of the dispersed gas phase. For the REG plate at high shaking frequencies however, i.e. 800 rpm, $k_L a_{app}$ values seem to decrease, rather than increasing. This is likely due to fluid vortexing, thus decreasing the height of liquid above the sparger and reducing the bubble residence time. Pluronic is a non-ionic surfactant that stabilises bubble formation which will therefore cause the bubbles to separate, thus increasing a and hence $k_L a$. However, the water–pluronic solution values, shown in Fig. 2, are most likely lower than values in actual culture media due to the presence of additional salts. Increasing salt concentration will decrease the mean bubble size [26], thus increasing a, hence leading to increased $k_L a$ values.

Various methods have been used to assess $k_L a$ values in shaken microwells. Doig et al. [7] used a dynamic gassing out method to measure $k_L a$ values and compared these to calculated values from the mass transfer limited growth rate of a strict aerobic micro organism. For a 24-well plate, fill volume of 1182 μL, orbital diameter from 3 to 8 mm and shaking frequencies from 200 to 900 rpm, $k_L a$ values were reported between 36 and 180 h^{-1}. Furthermore these authors established a correlation in order to predict $k_L a$ values in microwell systems as a function of fluid properties, shaking frequency and well geometry [7]. Hermann et al. [27] utilised the sulphite oxidation method to determine $k_L a$ values for a 96 well plate design, with reported values ranging from approximately 25–150 h^{-1}. For mammalian cell cultures, however, the oxygen demand is less severe [8]. Barrett et al. [10] reported values ranging from 1.1 to 29 h^{-1} for 24 SRW plates at shaking frequencies from 120 to 300 rpm. In comparison to stirred bioreactors Micheletti et al. [28] reports a value of 61.2 h^{-1} for a 3.5 L STR equipped with a 70 mm three-blade segment impeller at an agitation rate of 150 rpm

Table 2

Measured liquid phase mixing times for the REG plate design as a function of gas flow rate. Experimental conditions: stationary start; shaking frequency 500 rpm; d_o 2.5 mm; 7 mL fill volume; 25 °C. Errors represent one standard deviation about the mean ($n = 3$).

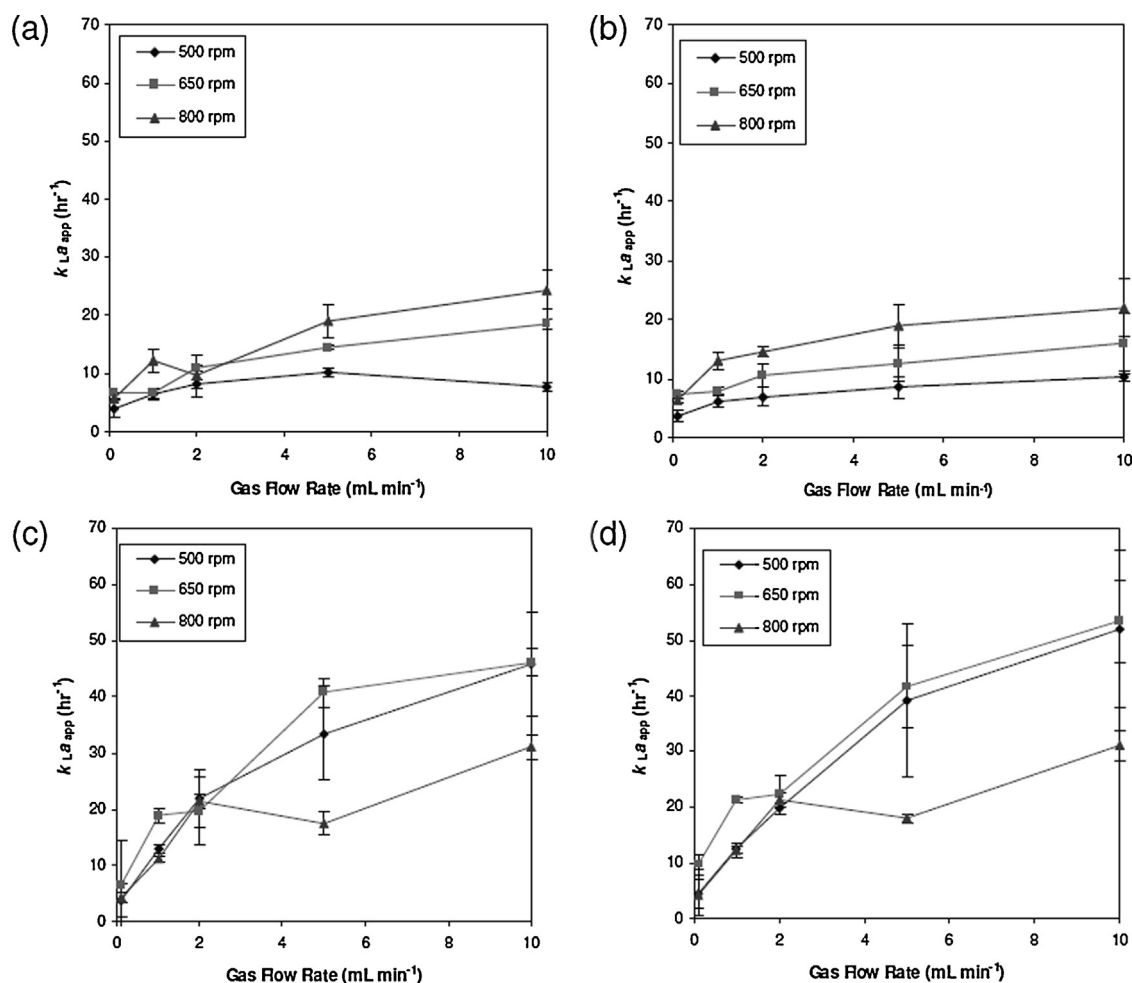| Gas flow rate (mL min^{-1})	Normalised gas flow rate (VVM)	Mixing time (s)
0	0.00	210 ± 78
0.2	0.03	59 ± 18
2	0.29	31 ± 7
4	0.57	26 ± 5
6	0.86	20 ± 5
8	1.14	12 ± 2
10	1.43	11 ± 2

Fig. 2. Apparent $k_L a$ values determined using the static gassing out method for (a and b) PERC and (c and d) REG plate designs with RO water containing $0.5\,g\,L^{-1}$ Pluronic F-68 and PPG media respectively. Experimental conditions: 7 mL fill volume; d_o 2.5 mm; 0.1–$10\,mL\,min^{-1}$ gas flow rates; shaking frequencies 500 (♦), 650 (■) and 800 rpm (▲). Error bars represent one standard deviation about the mean ($n = 3$). $k_L a$ values determined as described in Section 2.2.1.

and 0.1 VVM gas flow rate; whilst Tissot et al. [23] reports a value of $4\,h^{-1}$ for a 1.5 L STR employing a 45 mm pitched blade impeller and a gas flow rate of $0.3\,mL\,min^{-1}$ and agitation rates up to 150 rpm. Therefore, $k_L a_{app}$ values reported here ranging from 4–$22\,h^{-1}$ and 4–$53\,h^{-1}$ for media; and from 4–$24\,h^{-1}$ and 4–$46\,h^{-1}$ for water with $0.5\,g\,L^{-1}$ Pluronic solution for the PERC and REG plate designs respectively are within the ranges reported for similar systems. In terms of cell culture, specific oxygen uptake rates (qO_2) range from 2.3×10^{-17} to 1.7×10^{-16} mol oxygen cell^{-1} s^{-1} [29] and so $k_L a_{app}$ values of this magnitude would appear adequate to satisfy the oxygen transfer demands of most mammalian cell culture processes.

In order to understand how the available gas–liquid interfacial area impacts on the measured $k_L a_{app}$ values, the displaced liquid height was quantified by analysis of high speed camera images. For either plate design, the displaced liquid height increases by 17, 23 and 32 mm at agitation frequencies of 500, 650 and 800 rpm with gas–liquid interfacial areas of 220, 310 and $410\,mm^2$, respectively. Subsequently, the gas–liquid transfer area at the surface of the liquid was calculated based on these values. As expected, increasing the shaking frequency increases the displaced liquid height for both plate designs and thus the calculated liquid area in contact with the gas at the liquid surface. This reinforces the trends seen in $k_L a_{app}$ values indicating that increasing the shaking frequency increases the available gas–liquid transfer area and thus $k_L a_{app}$. For the PERC plate, where there is no dispersed gas phase, the relationship between a and $k_L a_{app}$ is almost linear over the range of shaking

frequencies tested. An increase in shaking frequency from 500 to 800 rpm is seen to approximately double the gas–liquid transfer area; leading to an approximate doubling in $k_L a_{app}$ (Fig. 2a and b). This indicates that the increases in $k_L a_{app}$ and hence oxygen transfer are primarily due to the increase in a while the fluid hydrodynamics have little influence on k_L. As seen in Fig. 1 the plate design also has little impact on the displaced liquid height and the available gas–liquid transfer area at the surface.

When the REG plate is aerated, Fig. 3 shows the nature of the gas–liquid dispersion produced. Visually this varies greatly between water (coalescing) or the water–pluronic solution and the two types of cell culture media (non-coalescing) studied. In all cases, there is no significant entrainment of the gas bubbles, but an 'imperfect bubbly' [30] flow regime; bubble packing is observed resulting in a 'foam' layer appearing at the surface; this phenomenon is less likely to occur in a traditional STR. This foam layer was observed to persist for up to 4 min; hence antifoam was used during all REG plate cell culture experiments.

Analysis of the number and size distribution of the dispersed gas bubbles produced is presented in Table 3. This indicates a complex series of interactions between media composition and the resultant gas phase characteristics in the bioreactor, which can be attributed to the presence of electrolytes in solution [31]. For example, in contrast to water, for the water–pluronic solution or either media, the mean bubble diameter d is smaller, therefore there are an increased number of bubbles and surface area, a,
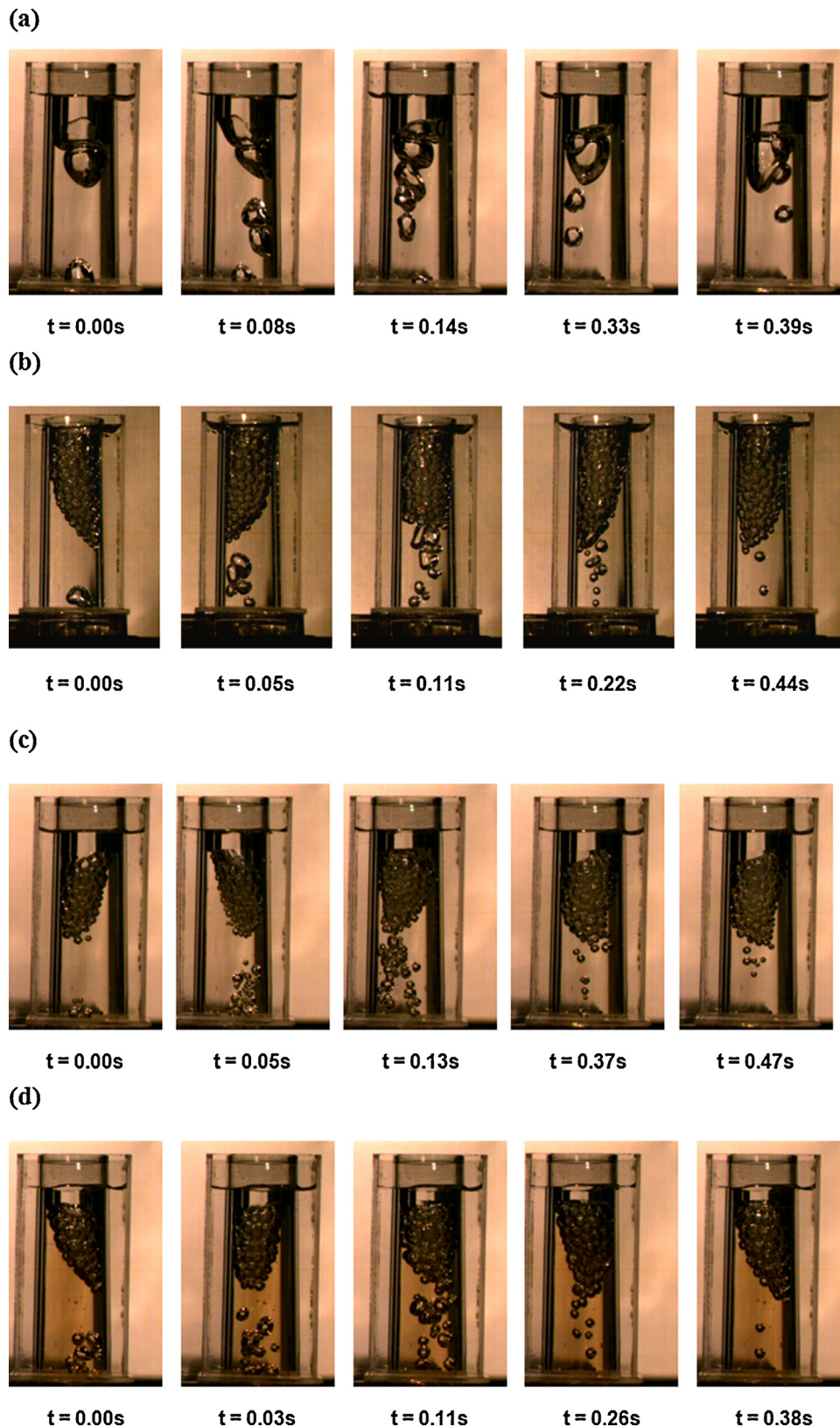
(a)

| t = 0.00s | t = 0.08s | t = 0.14s | t = 0.33s | t = 0.39s |

(b)

| t = 0.00s | t = 0.05s | t = 0.11s | t = 0.22s | t = 0.44s |

(c)

| t = 0.00s | t = 0.05s | t = 0.13s | t = 0.37s | t = 0.47s |

(d)

| t = 0.00s | t = 0.03s | t = 0.11s | t = 0.26s | t = 0.38s |

Fig. 3. Visualisation of gas bubble number and size distribution in the REG plate design for (a) water (b) water with 0.5 g L^{-1} Pluronic-F68, (c) CD-CHO media and (d) PPG. Experimental conditions: 7 mL fill volume; 650 rpm shaking frequency; d_o 2.5 mm; 5 mL min^{-1} gas flow rate.

available for oxygen transfer with each gas pulse. The bubble size will also be affected by the orifice diameter and the gas flow rate; in this case the high gas flow rate will dominate this relationship as observed by the relatively small gas bubbles produced [30]. The gas bubble size has a dramatic impact on energy dissipation as a result of gas bubble disengagement at the liquid surface [34]. Similarly, there is a progression to a decrease in average bubble residence time per pulse. For the different fluids tested, as residence times

Table 3
Analysis of gas bubble size, size distribution and volumetric gas hold up in the REG plate design for RO water (with/without 0.5 g L^{-1} Pluronic F-68), PPG and CD-CHO media. Experimental conditions: 7 mL fill volume; d_o 2.5 mm; 0.5 mL min^{-1} gas flow rate; shaking frequency 650 rpm. Values based on image analysis of high speed video images as shown in Fig. 3. Errors represent one standard deviation about the mean (n = 3).

Fluid	Bubbles per pulse	Mean bubble diameter, d (mm)	a (mm^2) per pulse	Bubble residence time (s)	Gas holdup per pulse (%, v/v)
Water	5.0 ± 0.1	4.8 ± 0.2	370	0.21 ± 0.06	4.4
Water + 0.5 g L^{-1} Pluronic F-68	22 ± 2	2.4 ± 1.1	410	0.11 ± 0.04	2.4
CD-CHO	56 ± 2	1.8 ± 0.5	560	0.15 ± 0.02	2.4
PPG	34 ± 4	2.9 ± 0.6	930	0.14 ± 0.02	6.5

change, the gas–liquid surface area changes inversely. Accordingly, there is relatively little difference between the media in terms of the total gas–liquid surface area available per gas pulse when averaged out over the pulse duration. It is worth noting that the gas bubble distribution and dynamics observed here will be rather different in an STR, due to impeller-induced bubble break-up and their subsequent interaction and coalescence [8].

3.1.3. Evaporation studies

Due to the extended culture periods required for cell culture, evaporation, particularly from small scale systems with low working volumes can be problematic leading to uncontrolled changes in metabolite levels and culture osmolality [12]. It has been reported that high osmolality conditions increase cell specific productivity [35] therefore evaporation effects need to be minimised to overcome these non-specific influences on culture performance. In the μ24 system, the cassette is positioned such that column 1 is closest to the fans that help control the environmental temperature and 6 is furthest away whilst rows A and D are at the outside of the plate. Each well on the μ24 plate has a cap, with a plastic check valve and sterile membrane barrier to help reduce evaporation. The specific fold evaporation values over 9 days of a simulated batch culture are shown in Fig. 4. It can be seen that not only is there very little culture volume reduction by evaporation over this time (average of 0.6% per day over the whole plate) but evaporation rates are generally consistent across the plate and less than 10% (v/v) overall.
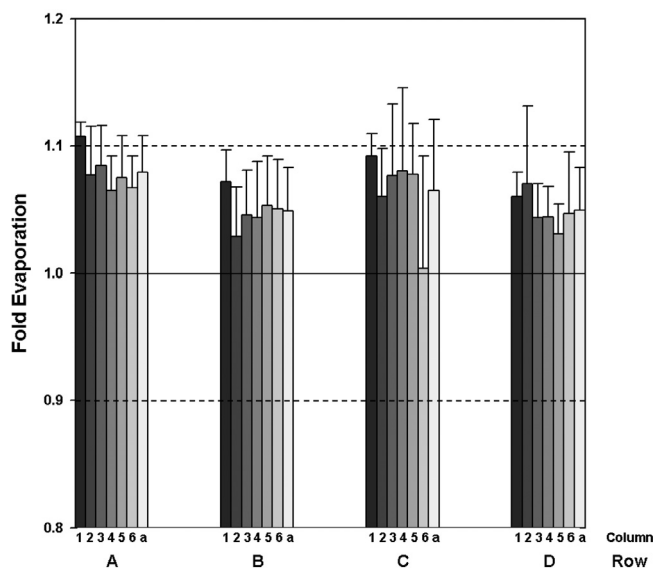

Fig. 4. Variation of evaporation per well across a μ24 PERC cassette during a typical batch culture period. Evaporation was measured as described in Section 2.2.3. Experimental conditions: Initial 0.002% (v/v) blue dye in RO water; 37 °C; 9 days duration; shaking frequency 650 rpm; d_o 2.5 mm; purge gas flow rate of 10 mL min^{-1}. Average (a) represents the mean with error bars indicating one standard deviation. Dashed lines represent ±10% variation about the mean.

3.2. μ24 cell culture kinetics

3.2.1. Achievement of consistent well-to-well performance

As shown in Supplementary Fig. 2(a) initial parallel batch cultures (n = 24) of the CHO $dhfr^{-/-}$ cell line in PERC plates showed considerable well-to-well variation even though all wells were controlled at the same set points. By day 8 the maximum VCD was 10.5×10^6 cells mL^{-1} and there was a maximum difference of 6.4×10^6 cells mL^{-1} equivalent to an 88% difference in final maximum and minimum VCD values. Subsequent experiments investigated ways to reduce this variability. Initial problems identified included inconsistent cell growth in some wells, either due to variation in the inoculum added or due to cell settling whilst sampling.

To counter these issues a microplate shaker was used to gently agitate the culture cassette when removed to a biological safety cabinet for sampling. In addition, a large volume, automated electronic pipette was employed to inoculate the wells in parallel. Using the optimised methodology cell culture kinetics across all wells were virtually identical as shown in Supplementary Fig. 2(b) and the final VCD increased to 19.3×10^6 cells mL^{-1}. There was no apparent systematic variation in performance across the plate with well-to-well variation in viable cell number reduced to less than 2.6×10^6 cells mL^{-1} at day 11, equivalent to a 14% difference in maximum and minimum VCD values.

3.2.2. Fed-batch cell culture kinetics in PERC plates

As shown in Section 3.2.1 the PERC plate design provides a homogeneous culture environment with adequate gas–liquid mass transfer for cell culture occurring solely via head space aeration. The detailed kinetic performance of 24 parallel fed-batch cultures of the CHO $dhfr^{-/-}$ cell line grown in PPG media under optimised conditions using the PERC plate is shown in Fig. 5(a). Under the conditions used the measured t_m during shaking was 2.0 s (Table 1) while the maximum $k_L a_{app}$ was approximately 8 h^{-1} (Fig. 2(b)).

As shown in Fig. 5(a, i) reproducible performance is again seen across all 24 wells. In terms of cell growth the peak cell density was almost 20.4×10^6 cells mL^{-1} at day 14 and viability remained above 60% for all wells. The on-line parameters (Fig. 5(a, ii)) demonstrate that the system was capable of maintaining all wells at their set points and that the control was reproducible across the culture cassette. DO was maintained at 57 ± 12% and pH at 6.95 ± 0.3. The spikes seen in the pH trace, for example at day 7, corresponds to manual sodium bicarbonate base feeding to readjust online pH. The metabolite data (Fig. 5(a, iii)) and antibody titre (Fig. 5(a, iv)) was shown to be consistent across the wells reaching a peak of approximately 1.6 g L^{-1} at day 14.

3.2.3. Fed-batch cell culture kinetics in REG plates

In contrast to the PERC plate, wells in the REG plate are individually aerated leading to the formation of a dispersed gas phase (Fig. 3). Using the REG plate format different gas operating strategies were investigated. The presence of the dispersed gas phase was believed to affect cell growth and antibody production [29]. In a traditional bioreactor a carrier gas is sparged through the culture in a
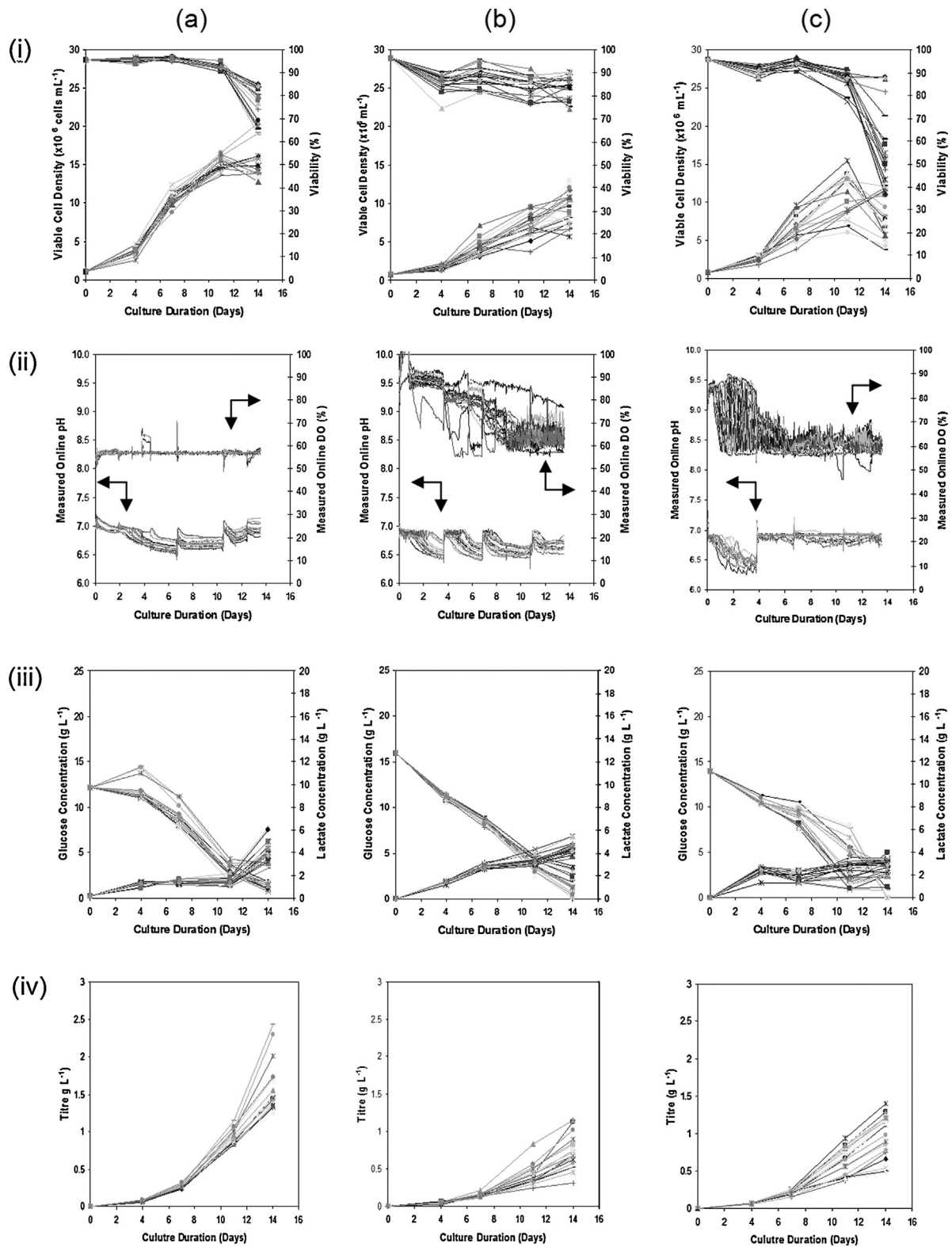
Fig. 5. Influence of plate design on 24 parallel fed-batch culture kinetics of a *dhfr*$^{-/-}$ cell line for (a) PERC plate, (b) REG plates operated in 'constant flow' mode, and (c) REG plates operated in 'active flow' mode: (i) VCD and viability (ii) online pH and DO values, (iii) glucose and lactate concentrations and (iv) mAb titre. Experimental conditions: d_o 2.5 mm; shaking frequency 650 rpm for the PERC plate and 550 rpm for the REG plate design. Experimental set points as described in Supplementary Fig. 2 and feeding performed as described in Section 2.4.2.

continuous manner, and other control gases, i.e. oxygen or carbon dioxide, are actively blended in as appropriate in order to control the system pH and DO set points. This aeration strategy was replicated in the μ24 'constant flow' protocol as reported in Section 2.4.2

and Supplementary Table 1, whereby air is constantly sparged at a desired flow rate, interspersed by the appropriate active sparging of gases to control pH (CO_2) and DO (40% O_2). In order to evaluate the effect of gas sparging on the system an 'active flow' protocol

Table 4
Derived growth parameters calculated from average cell culture data for shake flask, μ24 bioreactor using a PERC plate, and REG plate designs operated in a 'constant flow' or 'active flow' mode respectively, as described in Section 3.2.3.

System	Maximum IVC ($\times 10^6$ cells mL^{-1} day^{-1})	Cumulative IVC ($\times 10^6$ cells mL^{-1} day^{-1})	Instantaneous Q_p (pg cell^{-1} day^{-1})	Maximum volumetric productivity (mg L^{-1} day^{-1})	Maximum specific growth rate (day^{-1})	Maximum doubling time (day)
Shake flask	125	261	13.6	111	0.37	11.0
PERC 'constant flow'	128	253	14.4	113	0.34	7.7
REG 'constant flow'	62	119	12.2	53	0.32	8.7
REG 'active flow'	87	173	12.1	71	0.33	5.8

was also investigated as described in Section 2.4.2 and Supplementary Table 1. In this case no purge gas was used to constantly sparge the culture and therefore only 'active' sparging of gasses occurred in order to maintain pH and DO set points.

The performance of 24 parallel fed-batch cultures of the CHO $dhfr^{-/-}$ cell line in PPG media using the REG plate with either 'constant flow' or 'active flow' protocols is shown in Fig. 5(b) and (c) respectively. Under the operating conditions used the measured t_m values was approximately 7.0 s (Table 1) and the $k_L a_{app}$ was around 12 h^{-1} (Fig. 2(d)). The mean bubble size was 2.9 mm and the gas phase hold-up was 6.5% (v/v) (Table 3).

As shown in Fig. 5(b, i) the REG plate experiments operated using the 'constant flow' protocol again showed reproducible culture performance. The peak cell density was almost 12.9×10^6 cells mL^{-1} at day 14 and viability remained above 70% for all wells. Gassing in this case appeared to retard cell growth at the beginning of the growth phase, but the cells maintained a higher percentage viability over this time when compared to the PERC experiments. DO was maintained at $57 \pm 32\%$ and pH at 6.95 ± 0.4 (Fig. 5(b, ii)). Glucose and lactate concentrations were consistent across the parallel experiments (Fig. 5(b, iii)) and antibody concentration peaked at 1.15 g L^{-1} (Fig. 5(b, iv)).

In contrast, use of the 'active flow' protocol (Fig. 5(c, i)) showed a greater degree of variability in growth profiles. However, in general, there is good consistency across the wells in the plates, and the effect of bubble damage on cell culture performance is clearly shown. In this case the cell growth follows a pattern much more like that shown for the PERC plate, with a visible exponential growth phase, reaching a peak VCD of 15.5×10^6 cells mL^{-1} at day 11. However, after this point there is a more rapid decline in cell viability, leading to a final average viability below 60% at day 14. This can be explained due to the increased frequency in active gassing, at the higher cell densities, in order to control bioreactor set points. Online parameters are maintained with DO at $57 \pm 24\%$ and pH at 6.95 ± 0.2 (Fig. 5(c, ii)). Glucose and lactate concentrations follow cell growth, but with increased glucose utilisation and lactate production (Fig. 5(c, iii)). This is assumed to be because the cells are undergoing a greater degree of environmental stress, and are thus utilising more energy for cellular repair [32,33]. The peak antibody concentration was 1.40 g L^{-1} (Fig. 5(c, iv)).

Taken together these results highlight the significant impact that gas sparging has in small scale cell culture formats like the μ24. Energy dissipation rate increases rapidly with decreasing bubble size, e.g. in pure water for a bubble diameter of 6.32 mm energy dissipation is 10^5 W m^{-3} which increases to 10^8 W m^{-3} for a bubble diameter of 1.7 mm [29]. In comparison, the energy dissipation generated by an impeller which will have an approximate 10^1 W m^{-3} volume average for a typical animal cell bioreactor [29]. The constant gassing protocol appears to significantly retard cell growth at the exponential growth phase. However, this appears to condition the cells to the stress as a result of bubble damage. This is seen in the active gassing strategy; after approximately day 11 when there is a significant decrease in the viability of the cell population as a result of a significant increase in the frequency of gas sparging in

order to control the bioreactor set points at these now high cell densities.

Another issue that could be affecting cellular metabolism with regard to the different gassing strategies is that of CO_2 toxicity. It is widely believed that CO_2 build up is primarily an issue in large scale bioreactors where the increased hydrostatic pressure increases CO_2 solubility, and the low VVM gas flow rates that use an enriched oxygen air supply are unable to sufficiently strip the CO_2 and hence lead to cellular toxicity [8]. However, it is believed that this is not the cause of the lower VCD and titres exhibited by the REG plate cultures in 'constant flow' gas mode because of the small volume of the bioreactor system and that the 'constant flow' gassing regime would be stripping more CO_2 than that of the REG plate in the 'active flow' mode and thus the build up of dissolved CO_2 to toxic levels is unlikely to occur. Thus the reduced growth kinetics under the 'constant flow' regime is most likely solely attributed to the increased gas sparging frequency.

3.2.4. Comparison of μ24 and shake flask culture kinetics

In the previous section comparison of PERC and REG plate designs, under similar operating conditions (low t_m, adequate $k_L a_{app}$) showed that differences in cell culture performance were primarily attributed to the presence of the dispersed gas phase in the REG plates. Here the performance of the two plate designs is compared to conventional shake flask fed-batch cultures also at a matched mixing time ($\sim$6 s) as shown in Fig. 6.

As shown in Fig. 6(a) the cell growth kinetics in the PERC plates outperform those measured in the shake flask systems due to better control of culture parameters in the μ24. The observed higher antibody titre in the shake flask (Fig. 6(c)) is in fact not significant due to the overlapping error bars. The shake flask titre is believed to be similar to that of the PERC plate results due to the fact that the viability is lower and therefore incomplete antibody fragments will be released, thus over predicting the shake flask antibody titre value. The REG plate results are lower due to increased cellular stress as a result of gas sparging, and hence lower VCD values and lower product titre.

Derived growth parameters are calculated and presented in Table 4 for the four culture conditions. The integral viable cell (IVC) count shows the measure of viable cells in the culture at a given time point. The PERC plate has the highest maximum IVC, thus illustrating the capacity for this system to support the highest number of viable cells. Similarly, the PERC plate has the highest instantaneous cell specific productivity (Q_p) value. This highlights that the system is able to support a high number of cells, and also because of the monitoring and control capabilities, the cells also express a greater amount of product. The maximum specific growth rate reflects the cell growth data, with the growth rates in the REG plate lower than that of the PERC format. This also highlights the fact that the negative impact due to the cellular damage caused by the bubbles in the REG cultures has a greater impact than the positive impact of monitoring and controlling culture conditions.

Monitoring and control of culture parameters, pH and DO, in the μ24 as in conventional bench and production bioreactors, means that more representative data is obtained as opposed to other
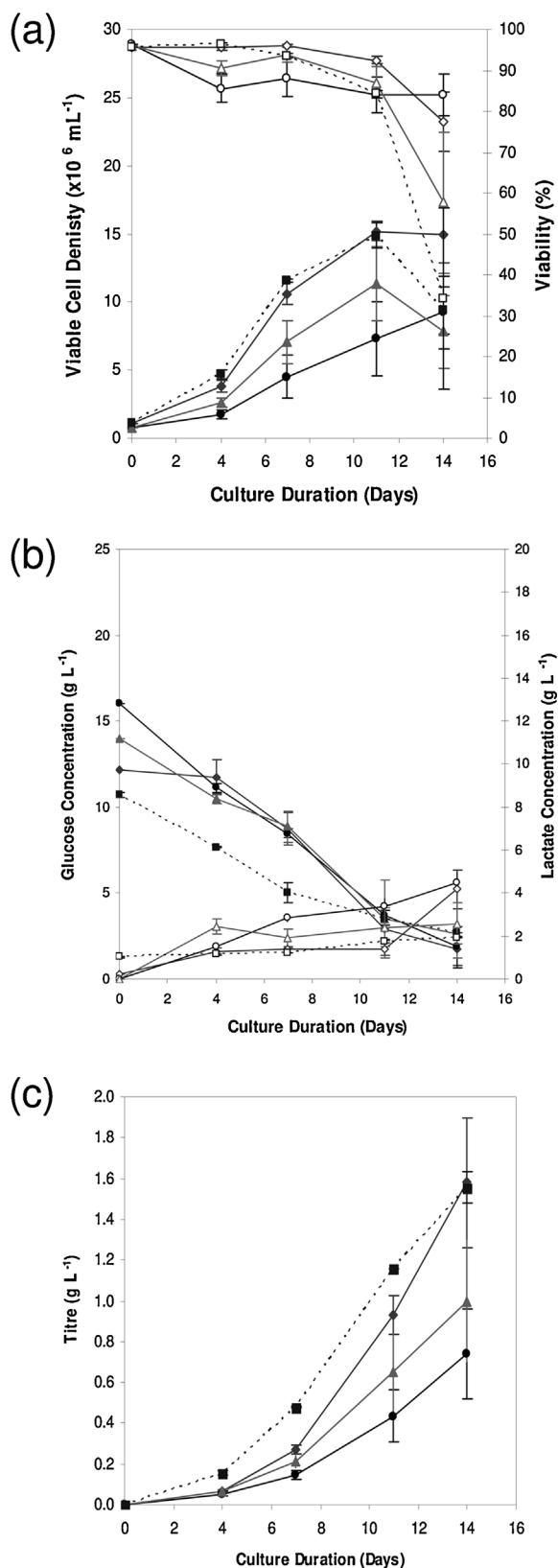
Fig. 6. Comparison of fed-batch culture kinetics of a *dhfr*$^{-/-}$ cell line between PERC ($\blacklozenge$, $\lozenge$) and REG plate designs operated in 'constant flow' mode ($\blacktriangle$, $\triangle$), and 'active flow' mode ($\bullet$, $\circ$). Reference shake flask data ($\blacksquare$, $\square$) indicated with dashed line: (a) VCD ($\blacklozenge$, $\blacksquare$, $\blacktriangle$, $\bullet$) and viability ($\lozenge$, $\square$, $\triangle$, $\circ$), (b) glucose ($\lozenge$, $\square$, $\triangle$ $\circ$) and lactate ($\blacklozenge$, $\blacksquare$, $\blacktriangle$, $\bullet$) concentrations and (c) mAb titre. The PERC and REG cultures were performed as described in Fig. 5 with shake flasks shaken at 250 rpm at a 25 mm orbital diameter. Error bars represent one standard deviation about the mean ($n = 24$ for μ24 data; $n = 6$ for shake flask data).

scale down formats, e.g. shake flasks, normal microtitre plates. The PERC plate design appears most suited to identifying very high VCD/producing cell lines, i.e. in the context of early stage clone screening and selection. However, for the REG plate, whilst relative culture performance was not as good; this design introduces a dispersed gas phase and so is expected to be more similar to conventional bioreactors. Therefore, when looking to devise a scale down mimic of a conventional STR the REG plate design may be preferable. Conditions in bench and production scale bioreactors are not uniform or constant engineering environments and do challenge cells to grow, therefore early screening of cells by introducing demanding processing conditions may actually be beneficial to aid early stage cell culture process development and identification of scaleable cell lines.

4. Conclusions

A full engineering characterisation of the μ24 bioreactor system was completed in this work to aid our fundamental understanding of how miniature bioreactor operating conditions impact on cell culture kinetics. Over a range of operating conditions both the PERC and REG plate designs were shown to be well mixed and demonstrated good control of environmental parameters like temperature and pH. Measured $k_L a_{app}$ values provided adequate oxygen transfer for DO to be maintained and controlled at acceptable levels. Successful application of the μ24 bioreactor was also demonstrated for a model cell line in terms of cell growth and productivity kinetics. Results in the REG plate were also reproducible but showed the impact the presence of a dispersed gas phase can have on cell culture performance.

Overall these results suggest that the μ24 can have a number of applications in industrial cell culture process development. The 'ideal' environment offered by the PERC plates appears best suited for cell line selection studies under precisely controlled suspension culture conditions. Here the small scale of the μ24 format offers around a 10–100 fold reduction in scale and approximately a threefold increase in throughput, in terms of laboratory footprint, compared to commonly used shake flask systems. In contrast, the presence of the dispersed gas phase in the REG plate design makes them more representative of a laboratory or pilot scale stirred bioreactor. The REG plate thus appears best suited for early stage cell culture process development studies and the ranking of clones under process relevant conditions.

Current work is examining the scalability of μ24 culture performance to conventional bench scale stirred tank bioreactors with a view to defining which plate design and operating strategy provides the best prediction of laboratory (2 L wv) and pilot (50 L wv) scale cell culture performance.

Appendix A. Supplementary data

Supplementary data associated with this article can be found, in the online version, at http://dx.doi.org/10.1016/j.bej.2013.11.010.

References

[1] S. Simoens, Health economics of market access for biopharmaceuticals and biosimilars, J. Med. Econ. 12 (2009) 211–218.

[2] R. Jefferis, Recombinant antibody therapeutics: the impact of glycosylation on mechanisms of action, Trends Pharmacol. Sci. 30 (2009) 356–362.

[3] B. Kelley, Industrialization of mAb production technology: The bioprocessing industry at a crossroads, MAbs 1 (2009) 443–452.

[4] A. Shukla, B. Hubbard, T. Tressel, S. Guhan, D. Low, Downstream processing of monoclonal antibodies – application of platform approaches, J. Chromatogr. B 848 (2007) 28–39.

[5] K. Sikora, Paying for cancer care – a new dilemma, J. R. Soc. Med. 100 (2007) 166–169.

[6] S. Farid, Process economics of industrial mAb manufacture, J. Chromatogr. B 848 (2007) 8–18.

[7] S.D. Doig, F. Baganz, G.L. Lye, High throughput screening and process optimisation, in: C. Ratledge, B. Kristiansen (Eds.), Basic Biotechnology, Cambridge University Press, Cambridge, 2006, pp. 289–306.

[8] A. Nienow, Reactor engineering in large scale animal cell culture, Cytotechnology 50 (2006) 9–33.

[9] N. Szita, P. Boccazzi, Z. Zhang, P. Boyle, A. Sinskey, K. Jensen, Development of a multiplexed microbioreactor system for high-throughput bioprocessing, Lab Chip 5 (2005) 819–826.

[10] T. Barrett, A. Wu, H. Zhang, S. Levy, G. Lye, Microwell engineering characterization for mammalian cell culture process development, Biotechnol. Bioeng. 105 (2010) 260–275.

[11] P. Girard, M. Jordan, M. Tsao, F. Wurm, Small-scale bioreactor system for process development and optimization, Biochem. Eng. J. 7 (2001) 117–119.

[12] N. Silk, S. Denby, M. Kuiper, D. Hatton, R. Field, F. Baganz, G. Lye, Fed-batch operation of an industrial cell culture process in shaken microwells, Biotechnol. Lett. 32 (2010) 73–78.

[13] R. Strobel, D. Bowden, M. Bracey, G. Sullivan, C. Hatfield, N. Jenkins, V. Vinci, High throughput cultivation of animal cells using shaken microplate techniques, in: E. Lindner-Olsson, N. Chatzissavidou, E. Lüllau (Eds.), Animal Cell Technology: From Target to Market, Kluwer, Dordrecht, The Netherlands, 2001, pp. 307–311.

[14] A. Chen, R. Chitta, D. Chang, A. Amanullah, Twenty-four well plate miniature bioreactor system as a scale-down model for cell culture process development, Biotechnol. Bioeng. 102 (2009) 148–160.

[15] K. Isett, H. George, W. Herber, A. Amanullah, Twenty-four-well plate miniature bioreactor high-throughput system: assessment for microbial cultivations, Biotechnol. Bioeng. 98 (2007) 1017–1028.

[16] K. van't Riet, Review of measuring methods and results in nonviscous gas–liquid mass transfer in stirred vessels, Ind. Eng. Chem. Proc. Des. Dev. 18 (1979) 357–364.

[17] I.J. Dunn, A.J. Einsele, Oxygen transfer coefficients by the dynamic method, J. Appl. Chem. Biotechnol. 25 (1975) 707–720.

[18] W. Bujalski, K. Takenaka, S. Paolini, M. Jahoda, A. Paglianti, K. Takahashi, A.W. Nienow, A.W. Etchells, Suspension and liquid homogenization in high solids concentration stirred chemical reactors, Chem. Eng. Res. Des. 77 (1999) 241–247.

[19] A.J. Nealon, R.D. O'Kennedy, N.J. Titchener-Hooker, G.J. Lye, Quantification and prediction of jet macro-mixing times in static microwell plates, Chem. Eng. Sci. 61 (2006) 4860–4870.

[20] N. Silk, High Throughput Approaches to Mammalian Cell Culture Process Development, University College London, 2012, EngD Thesis.

[21] H. Büntemeyer, Methods for off-line analysis of nutrients and products in mammalian cell culture, in: R. Pörtner (Ed.), Methods in biotechnology Animal Cell Biotechnology: Methods and Protocols, 24, Humana Press Inc., Totowa, NJ, 2007, pp. 253–268.

[22] J. Büchs, S. Lotter, C. Milbradt, Out-of-phase operating conditions, a hitherto unknown phenomenon in shaking bioreactors, Biochem. Eng. J. 7 (2001) 135–141.

[23] S. Tissot, A. Oberbek, M. Reclari, M. Dreyer, D.L. Hacker, L. Baldi, M. Farhat, F.M. Wurm, 2011. Efficient and reproducible mammalian cell bioprocesses without probes and controllers? New Biotechnol. 28 (2011) 382–390.

[24] A. Nienow, On impeller circulation and mixing effectiveness in the turbulent flow regime, Chem. Eng. Sci. 52 (1997) 2557–2565.

[25] G. Catapano, P. Czermak, R. Eibl, D. Eibl, R. Pörtner, Bioreactor design and scale-up, in: R. Eibl, D. Eibl, R. Pörtner, G. Catapano, P. Czermak (Eds.), Cell and Tissue Reaction Engineering., Springer Berlin Heidelberg, Berlin, 2009, pp. 173–259.

[26] J. Villadsen, J. Nielsen, G. Lidén, Bioreaction Engineering Principles, Springer, New York, 2011, pp. 459–496.

[27] R. Hermann, M. Lehmann, J. Büchs, Characterization of gas–liquid mass transfer phenomena in microtiter plates, Biotechnol. Bioeng. 81 (2003) 178–186.

[28] M. Micheletti, T. Barrett, S. Doig, F. Baganz, M. Levy, J. Woodley, G.J. Lye, Fluid mixing in shaken bioreactors: implications for scale-up predictions from microlitre-scale microbial and mammalian cell cultures, Chem. Eng. Sci. 61 (2006) 2939–2949.

[29] R. Godoy-Silva, C. Berdugo, J. Chalmers, Aeration Mixing and hydrodynamics, animal cell bioreactors, in: M. Flickinger (Ed.), Encyclopedia of Industrial Biotechnology: Bioprocess Bioseparation, and Cell Technology, Wiley, New York, 2010, pp. 1–27.

[30] N. Kantarci, F. Borak, K.O. Ulgen, Bubble column reactors, Process Biochem. 40 (2005) 2263–2283.

[31] S. Sideman, Ö. Hortaçsu, J.W. Fulton, Mass transfer in gas–liquid contacting systems, Ind. Eng. Chem. 58 (1966) 32–47.

[32] C. Heath, R. Kiss, Cell culture process development: advances in process engineering, Biotechnol. Progr. 23 (2007) 46–51.

[33] Y. Ho, J. Varley, A. Mantalaris, Development and analysis of a mathematical model for antibody-producing GS-NS0 cells under normal and hyperosmotic culture conditions, Biotechnol. Progr. 22 (2006) 1560–1569.

[34] M. Al-Rubeai, S.K.W. Oh, R. Musaheb, A.N. Emery, Modified cellular metabolism in hybridomas subjected to hydrodynamic and other stresses, Biotechnol. Lett. 12 (1990) 323–328.

[35] S.K.W. Oh, A. Nienow, M. Al-Rubeai, A.N. Emery, The effects of agitation intensity with and without continuous sparging on the growth and antibody production of hybridoma cells, J. Biotechnol. 12 (1989) 45–62.